Spin wave propagation in spatially nonuniform magnetic fields

Kevin R. Smith,[1,2,a)] Michael J. Kabatek,[1] Pavol Krivosik,[1,3] and Mingzhong Wu[1,b)]
[1]*Department of Physics, Colorado State University, Fort Collins, Colorado 80523, USA*
[2]*Agilent Technologies, Englewood, Colorado 80112, USA*
[3]*Slovak University of Technology, 812 19 Bratislava, Slovakia*

(Received 27 March 2008; accepted 30 May 2008; published online 22 August 2008)

Spin wave pulse propagation in a magnetic thin film under static, spatially nonuniform magnetic fields has been studied. The experiment was carried out with an yttrium iron garnet film strip. The film strip was magnetized with a spatially nonuniform magnetic field parallel to the length of the film strip. Spin wave pulses were excited with a microstrip transducer at one end of the film strip. The spin wave pulse propagation along the film strip was mapped with a high-resolution time- and space-resolved inductive magnetodynamic probe. The wave number for the spin wave pulses was found to increase in a spatially increasing field and decrease in a spatially decreasing field. The wave number change in a static, general spatially varying static field is reversible for this field-film geometry. The phase velocity was found to decrease in a spatially increasing magnetic field and increase in a spatially decreasing field. The carrier frequency of the spin wave pulses remained constant throughout pulse propagation. © *2008 American Institute of Physics*.
[DOI: 10.1063/1.2963688]

I. INTRODUCTION

Spin wave excitations in magnetic materials have attracted vigorous research over the last 60 years. The study of spin waves is fundamentally important for understanding many linear and nonlinear effects in magnetic systems. It is also important for the development of microwave devices such as phase shifters, delay lines, and frequency selective power limiters.[1–3] Most of the previous works concern spin wave excitations in spatially uniform magnetic fields. Only a limited amount of work has been done on spin wave propagation in nonuniform fields. Spin waves in nonuniform fields, however, are of great interest. There are two main reasons. First, the magnetic fields in spin wave research and applications are often not exactly uniform. Second, spin waves in strongly nonuniform fields have unique properties that could lead to novel device applications. The potential for device applications has stimulated various experimental and theoretical studies. They include coupling between the spin waves and elastic waves through the nonuniform demagnetizing fields[4–20] and the modification of spin wave propagation characteristics, such as dispersion, loss, group delay, and trajectory.[21–37]

The key idea behind nonuniform field-based spin wave devices lies in the spin wave wave number depending on the local value of the static magnetic field. Schlömann was the first to point out that the wave number of a spin wave propagating in a spatially nonuniform magnetic field should change with the magnitude of the field. Specifically, Schlömann[5] proposed to use the nonuniform demagnetizing fields at either end of a yttrium iron garnet (YIG) rod to couple elastic waves with spin waves. Explicit demonstration of this idea, however, has not been given until now.

This article presents the first experimental data on the spatial wave number change in spin waves propagating in spatially nonuniform magnetic fields. Specifically, the article reports on time- and space-resolved measurements of spin wave pulse propagation properties in a magnetic film strip that is magnetized to saturation with static, spatially nonuniform magnetic fields. The experiment was performed with a long and narrow magnetic YIG film strip. The spatially nonuniform fields were applied parallel to the long direction of the film strip. This film/field configuration corresponds to the propagation of backward volume spin waves (BVSWs).[2,3] The frequency versus the wave number dispersion relationship for the BVSW configuration depends on the magnetic field strength, saturation magnetization, and thickness of the magnetic film. A change in the magnetic field can shift the frequency versus the wave number dispersion curve up or down such that, for a given frequency, the wave number is different for a different field.

In this work, it is found that in a spatially nonuniform magnetic field, some of the BVSW pulse characteristics are set by the *local* magnetic field. Specifically, the wave number increases and the phase velocity decreases in a spatially increasing magnetic field, while the opposite occurs in a spatially decreasing magnetic field. Moreover, if the field first decreases and then returns to its initial strength, the wave number will do the same. The change in the wave number with field is therefore a reversible process. In spite of the changes in the wave number, the spin wave pulse carrier frequency remains constant throughout the pulse propagation. The group velocity is found to remain relatively constant for small changes in field.

Section II of this paper describes the experimental setup and measurement technique. Section III provides experimental results, analysis, and comparisons with work in the same vein. Section IV gives a brief summary of the present work.

[a)]Electronic mail: kevsmith@lamar.colostate.edu.
[b)]Author to whom correspondence should be addressed. Electronic mail: mwu@lamar.colostate.edu.

 © 2008 American Institute of Physics

Downloaded 26 Aug 2008 to 129.82.140.121. Redistribution subject to AIP license or copyright; see http://jap.aip.org/jap/copyright.jsp

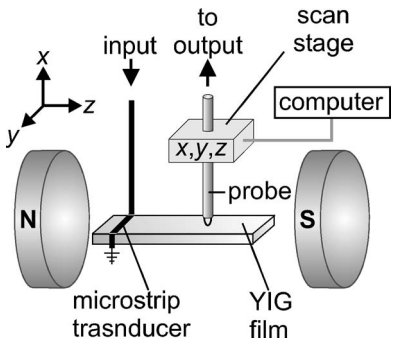

FIG. 1. Schematic diagram of the time- and space-resolved spin wave probe system. A microstrip transducer is used to excite spin wave pulses in the YIG film strip. A computer controlled *x*-*y*-*z* scan stage moves the inductive probe over the center of the strip along the long axis to detect the spin wave signal. An electromagnet, with adjustable pole pieces, provides the magnetic field.

II. EXPERIMENTAL SETUP AND MEASUREMENT TECHNIQUE

The experiment used a time- and space-resolved inductive probe system.[38] Figure 1 shows a schematic of the measurement system. A YIG thin film strip was magnetized by a field parallel to the length of the film strip. The YIG film was nominally 7.2 μm thick, 2 mm wide, and 11 mm long. A microstrip transducer was positioned at one end of the film strip for the excitation of spin wave pulses in the film strip. A magnetodynamic inductive loop probe was scanned just above the center of the film along its long axis to detect a spin wave pulse signal during its propagation. The inductive probe used in the experiment was sensitive to wave numbers up to 400 rad/cm. A computer controlled *x*-*y*-*z* scan stage was used to move the probe accurately.

The output time trace signal from the probe at every spatial point was recorded by using fast broadband microwave oscilloscope with a temporal resolution of 25 ps. The time-resolved signals at different positions along the long axis of the YIG film were accumulated to construct the spatiotemporal responses of the spin waves.

The spin wave pulses were excited with input microwave pulses with a temporal width of 35 ns and a carrier frequency of 5.515 GHz. This frequency is about 60 MHz below the BVSW cutoff frequency for the magnetic field near the input transducer. The nominal input power applied to the transducer was 32 mW, which was small enough to keep the spin wave pulses in the linear, nonsolitonic regime,[39] but large enough to provide detectable output signals.

The experiment was performed with three specific spatially nonuniform field configurations. The different configurations were realized through the adjustment of the positions of the two electromagnetic poles relative to the film/transducer structure. A standard Hall effect magnetic field detector, which was mounted on the scan stage in place of the inductive probe, was used to map the spatially nonuniform magnetic field H as a function of the distance z from the input transducer. The three $H(z)$ configurations consisted of fields that (i) increase with z, (ii) decrease with z, and (iii) have a decrease followed by an increase or a sag.

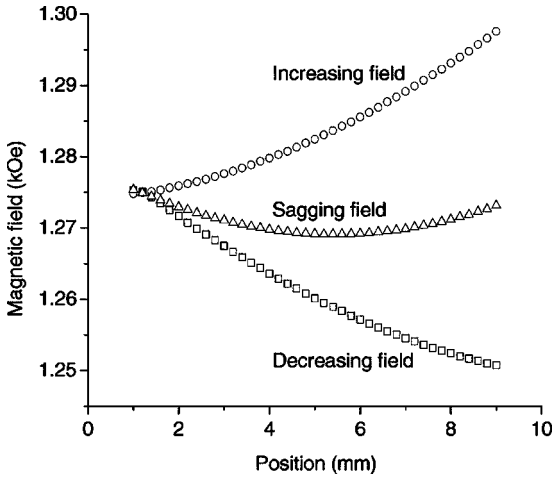

FIG. 2. Three magnetic field configurations. The magnetic field H is shown as a function of position z, which is the distance from the input transducer.

Figure 2 gives the actual static field $H(z)$ profiles utilized in the experiment. For both the increasing and decreasing field configurations, the overall field change over the length of the strip was about 20 Oe. For the sagging configuration, the maximum field change was about 5 Oe. Although the field change in all three configurations is relatively small compared to the nominal values, the data below clearly show that it is sufficient to produce significant changes in the carrier wave numbers and consequently the phase velocities for the spin wave pulses. The input pulse carrier frequency and the magnetic field at the input transducer position, i.e., for $z=0$, have been chosen in order to obtain a moderate value of the initial carrier wave number. This initial value ensured that the spin wave pulse wave number stayed within the bandwidth of the inductive probe.

III. EXPERIMENTAL RESULTS AND ANALYSIS

Figure 3 shows a small section of a spatiotemporal map of a spin wave pulse that propagated through the decreasing field configuration. It was constructed as described in the previous section. The vertical axis shows the propagation distance z in millimeters, while the horizontal axis shows delay time in nanoseconds. The color indicates the voltage induced in the inductive probe. Dark red represents the highest induced voltage, while dark blue represents the largest negative induced voltage. Light green indicates the areas where no voltage signals are detected. The data are normalized to the largest positive voltage. The dashed black vertical and horizontal lines represent slices of space and time, respectively. The left box shows a generic spatial waveform for the vertical slice. The top box shows a generic temporal waveform of the slice indicated by the horizontal line. The solid black line indicates the phase fronts of the spin wave in the space-time domain. The black arrow to the right of the figure indicates the direction of the decreasing magnetic field.

A vertical slice of this spatiotemporal map represents the spatial portion of the spin wave for that instance in time. Similarly, a horizontal slice represents the time-domain signal at that position in space. A Fourier transform can be

Downloaded 26 Aug 2008 to 129.82.140.121. Redistribution subject to AIP license or copyright; see http://jap.aip.org/jap/copyright.jsp

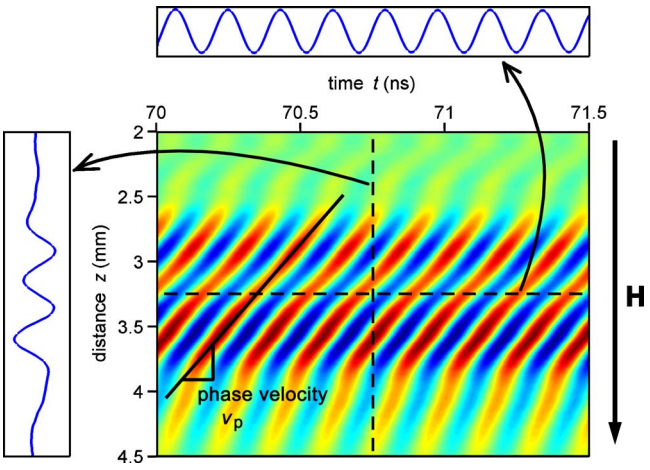

FIG. 3. (Color online) Spatiotemporal map for the propagation of a spin wave pulse. These data were obtained with the inductive probe for the decreasing field configuration. Red corresponds to positive voltage, while blue corresponds to negative voltage. Green represents no voltage. The data are normalized to the largest positive voltage. The vertical and horizontal dashed lines represent slices in the space and time domains for a given instance and position, respectively. The left and top boxes represent typical slices, as indicated. The large arrow to the right indicates the direction of the magnetic field. The diagonal black line in the figure represents the phase front of the spin wave pulse.

performed on either the vertical or horizontal slice, the peak of which gives the wave number and the carrier frequency for that instance in time and space, respectively. The slope of the phase front can be taken as the phase velocity. All of the data presented later are taken from spatiotemporal maps similar to that in Fig. 3.

Figure 4 shows the spatial evolution of BVSW pulses for

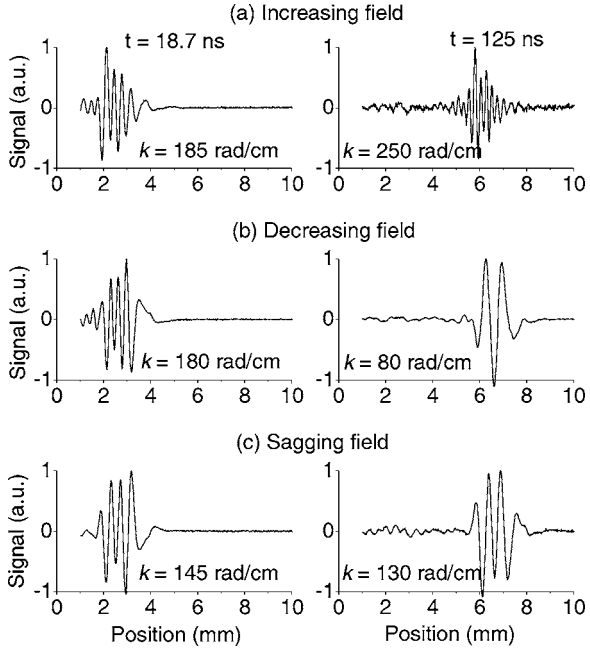

FIG. 4. Spatial evolution of spin wave pulses for three different field configurations. Normalized spin wave pulse waveforms are shown in the space domain at two different times for the three nonuniform field configurations, as shown in Fig. 2. The waveforms in the left column were taken at 18.7 ns after launch, and those in the right column were taken at 125 ns. The wave number of each pulse is shown.

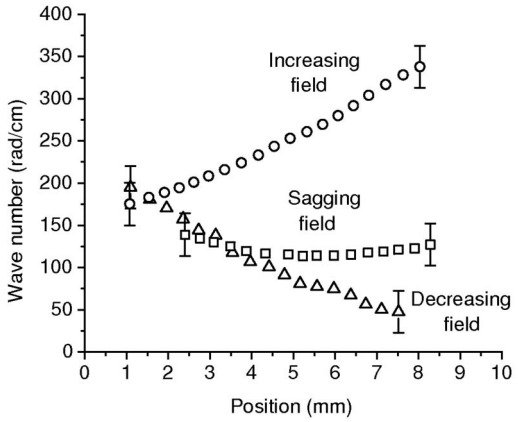

FIG. 5. Spin wave wave number as a function of spin wave propagation distance. The data are for the increasing field, decreasing field, and sagging field configurations, as indicated. The error bars are for all of the data.

the three different field configurations shown in Fig. 2. The plots show normalized spin wave signals as a function of position at two different time instances. The spatial dependences were obtained from the spatiotemporal propagation maps constructed in the way described above. The waveforms in the left column correspond to time $t=18.7$ ns, relative to the launch of the initial pulse to the input microstrip transducer, while those in the right column were taken at $t=125$ ns. The wave number of each pulse was obtained from spatial fast Fourier transform of the signals and is indicated in each graph. The input microwave pulses for all the configurations had the same carrier frequency, temporal width, and power as given above.

The data given in Fig. 4 show the general wave number trend for BVSW pulses that propagate in static, spatially nonuniform magnetic fields. The data in (a) for an increasing field show that, after over propagation of about 4 mm or 106 ns, the pulse carrier wave number increases significantly. An analysis of the waveforms shows an *increase* from about 175 rad/cm at about 2–3 mm to nearly 275 rad/cm at about 6 mm. In contrast, the data in graph (b) for a decreasing field show a significant *decrease* in the carrier wave number. Here, the change is from 175 rad/cm at about 2–3 mm to 50 rad/cm at about 6–7 mm. The two waveforms in (c) for a sagging field, however, show similar carrier wave numbers at both of the time points. Note that, for the data in graph (c), one has $H \approx 1270$ Oe at both the 2–3 and 6–7 mm positions. These data show that for the 106 ns propagation time, each pulse has traveled nearly the same distance, yielding one and the same group velocity of 3.7×10^6 cm/s. This group velocity is in good agreement with theoretical estimation for BVSW configuration.[2,3] The data in Fig. 3 also show that, in all three cases, the spatial width of the spin wave pulses remains more or less constant in spite of the nonuniform $H(z)$.

Figure 5 summarizes results on the wave number k versus the position z dependence for all three $H(z)$ configurations. The empty squares represent data for the increasing field configuration, while the empty circles represent the data for the decreasing field. The sagging field data are represented by triangles. The overall propagation distance was about 8 mm. Data are shown for distances greater than 1 mm

Downloaded 26 Aug 2008 to 129.82.140.121. Redistribution subject to AIP license or copyright; see http://jap.aip.org/jap/copyright.jsp

only since the probe could not be positioned any closer to the input transducer. For these data, the spatial waveforms at a series of time moments were first determined from the time-domain measurements. A fast Fourier transform was then performed on the spatial waveforms at each point in time, and the central wave number was obtained. Each time point was multiplied by the measured group velocity to obtain the spatial position of the pulses. The error bars are for the whole data range and are ± 25 rad/cm.

The data in Fig. 5 quantitatively show the observations on the wave numbers noted above. The data for the increasing field clearly show that the wave number k increases with z for an increasing field $H(z)$, while the data for the decreasing field show that the wave number k decreases with z for a decreasing field $H(z)$. Both show net wave number changes greater than 100 rad/cm, from $z=1$ mm to $z=8$ mm. The data for the sagging field, on the other hand, show that k first decreases and then increases, or sags, with z for a sagging magnetic field $H(z)$ configuration. The net wave number change from $z=1$ mm to $z=7$ mm is nearly zero.

Taken together, Figs. 4 and 5 show that the wave number of a BVSW pulse largely depends on the strength of the local magnetic field. For a spatially increasing field, the wave number increases, and for a spatially decreasing field, the wave number decreases. The data for the sagging field configurations in both Figs. 4 and 5 show another important fact, namely, that the process is reversible.

These magnetic field versus wave number responses occur because the BVSW frequency versus the wave number dispersion relation explicitly depends on the magnetic field H. The BVSW dispersion relation in the magnetostatic limit is given by[2,3]

$$\omega(k) = |\gamma| \sqrt{H^2 + H 4\pi M_s \left(\frac{1 - e^{-kd}}{kd} \right)}, \tag{1}$$

where ω is the angular carrier frequency, k is the carrier wave number, γ is the gyromagnetic ratio, M_s is the saturation magnetization, and d is the film thickness. This dispersion relation $\omega(k)$ is a decreasing function of the wave number k. For a given carrier frequency, therefore, an increase in the magnetic field strength H results in an upshift of the dispersion curve and thereby an increase in the wave number. Similarly, a decrease in the magnetic field strength leads to a downshift of the dispersion curve and thereby a decrease in the wave number. For the nonuniform fields presented in this work, the magnetic field may be taken as a function of the distance from the transducer z.

Figure 6 explicitly demonstrates the main point of this article: The carrier wave number of a spin wave depends on the local magnetic field. The empty circles and squares show the combined data from Figs. 2 and 5 in the wave number k versus the static magnetic field H format for the increasing and decreasing field configurations, respectively. For clarity, the sagging field configuration data are not shown. The straight solid line is a fit to the data based on a linearized form of Eq. (1), obtained by the expansion of the exponential, for film thicknesses of 7.2 μm and a saturation induction $4\pi M_s$ 1750 G and an additional 40 Oe of anisotropy. The horizontal error bars for the static field are representative of the whole field range.

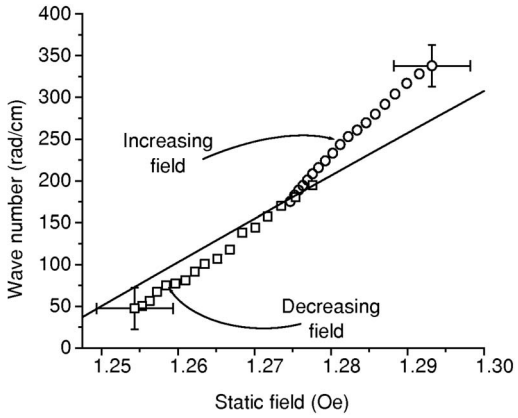

FIG. 6. Spin wave wave number vs magnetic field. These data were taken from Figs. 2 and 4. The solid line is a theoretical fit to the data based on Eq. (1). The error bars are for the whole range of static field H and wave numbers.

The theoretical line shows a relatively good fit to the data for both field configurations. These data conclusively show that the wave number of a BVSW pulse depends monotonically on the local magnetic field in a nearly linear manner for wave numbers up to at least 400 rad/cm. It is clear that one can manipulate the wave number of the BVSW pulse through the local magnetic field.

It is important to note that these results are for $H(z)$ profiles in which the overall change in field was relatively small and gradual, and that the fields are always colinear with the strip length. As a consequence of the small field changes, the slope and curvature of the frequency versus the wave number dispersion curve do not change significantly. Therefore, the group velocity and spatial and temporal widths of the spin wave pulse are relatively the same for all of the configurations.

It is also important to note that the results presented here for spatially small field changes are different from those for large field changes. As presented in Ref. 37, spin waves could either tunnel through or be reflected by a local magnetic field barrier. The field barrier was created by a dc current carrying wire positioned over the surface and across the width of a YIG film strip. The spin wave tunneling is similar to quantum tunneling. The spin wave reflection occurs when the field in the sagging region is so small that the entire dispersion curve is shifted to be below the carrier frequency of the incident spin wave pulse.

In contrast with the $k(z)$ results discussed above, it is found that the carrier frequency of the spin wave pulses is unaffected by the field changes. This frequency result was determined from the fast Fourier transforms of the time-domain signals as a function of the propagation distance z. Figure 7 shows the central Fourier component of the propagating BVSW signals as a function of distance z. The empty squares represent data for the increasing field configuration, while the empty circles represent the data for the decreasing field. The dashed line shows the nominal input frequency of 5.515 GHz as a point of reference.

Downloaded 26 Aug 2008 to 129.82.140.121. Redistribution subject to AIP license or copyright; see http://jap.aip.org/jap/copyright.jsp

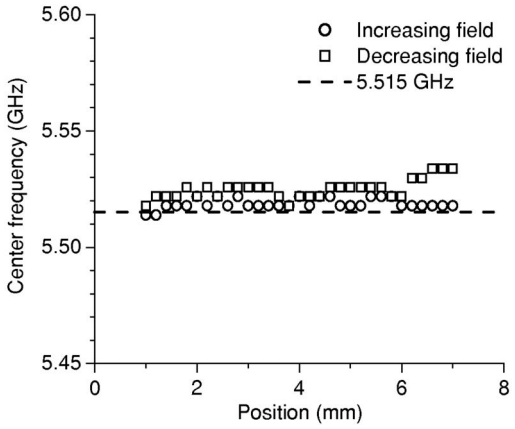

FIG. 7. Center frequency of spin wave pulses vs propagation distance. The data were obtained with temporal fast Fourier transforms of the output time-domain signals. The empty squares represent data for the increasing field configuration, while the empty circles represent the data for the decreasing field. The dashed line shows the nominal input frequency of 5.515 GHz.

These data show that the central carrier frequency of the BVSW pulses remains constant, while the pulses propagate through the spatially increasing or decreasing fields. This result is significant. It means that the spin wave pulses will maintain the same carrier frequency even as they propagate in a spatially changing field environment. The carrier frequency does not change because there are no temporal changes in the magnetic field. This constant frequency property should be contrasted with the case of spatially uniform but nonstationary (i.e., nonstatic) external magnetic fields. In general, nonstationary external fields change the carrier frequency.[40–42]

The data in Figs. 4–7 have shown that when a BVSW pulse propagates through a spatially nonuniform magnetic field the carrier wave number changes, while the carrier frequency remains constant. These two results indicate that the phase velocity can also be controlled in a predictable manner. Figure 8 shows representative BVSW phase velocity data as a function of distance z for the increasing and decreasing field conditions. The empty symbols denote data obtained from the slopes of the wave fronts in the space-time maps, as shown in Fig. 3. The solid symbols are data obtained as a ratio of spin wave frequency and measured wave number according to $\nu_p=\omega/k$, where the frequency $\omega/2\pi$ is 5.515 GHz and the wave number k was taken from the data in Fig. 5. The error bars for the wave front data are the size of the symbols.

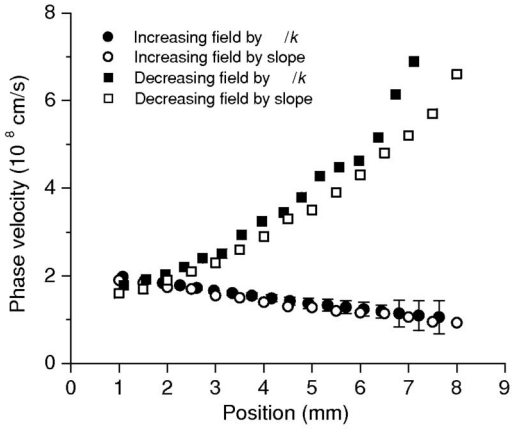

FIG. 8. Phase velocity of spin waves vs propagation distance. The phase velocity is shown for spatially increasing and decreasing fields, as indicated. The solid symbols were obtained from the standard phase velocity equation, $\nu_p=\omega/k$, where ω is the angular carrier frequency and k is the carrier wave data presented in Fig. 4. The empty symbols were obtained by measuring the slopes of the wave fronts in the space-time map. Error bars for the wave front data are the size of the symbols.

The data shown in Fig. 8 confirm expected behavior for the phase velocity of BVSW pulses that propagated in a spatially nonuniform magnetic field, i.e., inverse dependence of phase velocity with respect to wave number. The graphs also show a reasonable match of the data points obtained by the phase velocity formula and those obtained from the slopes of the wave fronts.

The results shown in Fig. 8 indicate that the phase velocity can be controlled by the local magnetic field through the adjustment of the carrier wave number. It should also be noted that the phase velocity of spin waves was never measured previously.

It is important to emphasize that these results are for the specific case of backward volume spin waves. The response would be exactly opposite in the case of surface and forward volume spin waves.[2,3] In these two cases, the spin wave frequency versus the wave number dispersion relation, $\omega(k)$, is an increasing function of k. The wave number should therefore increase in the spatially decreasing field and decrease in the spatially increasing field. It will be important to examine the spin wave propagation dynamics for the gamut of possible magnetic field configurations and the wide range of $\omega(k)$ responses that can be achieved by these variations.

Large field changes and propagation geometry variations may be useful for wave number manipulation, group and phase velocity control, and dispersion management, not to mention options for the tuning of nonlinear magnetodynamic response. These effects have important possibilities for new classes of microwave devices for signal processing applications.

IV. SUMMARY

High-resolution time- and space-resolved imaging of spin wave pulse propagation under spatially nonuniform magnetic fields has been realized with an inductive magnetodynamic probe. It is found that in a nonuniform field, the carrier wave number and phase velocity change, while the carrier frequency remains constant. Specifically, the wave number increases in the spatially increasing field and decreases in the spatially decreasing field, and this change is reversible for a general re-entrant field change. These field dependent wave number and phase velocity properties present potential microwave signal processing applications, such as novel delay lines, wave number selective devices, dispersion control devices, millimeter wave compression and expansion devices, and chirp control devices.

Downloaded 26 Aug 2008 to 129.82.140.121. Redistribution subject to AIP license or copyright; see http://jap.aip.org/jap/copyright.jsp

ACKNOWLEDGMENTS

This work was supported in part by the U.S. Army Research Office MURI (Grant No. W911NF-04-1-0247), the Office of Naval Research (Grant No. N00014-06-1-0889), and the National Science Foundation (Grant No. ECCS-0725386). Professor Carl E. Patton is gratefully acknowledged for providing the resources and useful discussions.

[1] J. D. Adam, S. N. Stitzer, and R. M. Young, IEEE MTT-S Int. Microwave Symp. Dig. **2**, 1173 (2001).
[2] P. Kabos and V. S. Stalmachov, *Magnetostatic Waves and Their Applications* (Chapman and Hall, London, 1994).
[3] D. D. Stancil, *Theory of Magnetostatic Waves* (Springer-Verlag, New York, 1993).
[4] P. C. Fletcher and C. Kittel, Phys. Rev. **120**, 2004 (1960).
[5] E. Schlömann, in *Advances in Quantum Electronics*, edited by J. R. Singer (Columbia University Press, New York, 1961), p. 445.
[6] J. R. Eshbach, Phys. Rev. Lett. **8**, 357 (1962).
[7] J. R. Eshbach, J. Appl. Phys. **34**, 1298 (1963).
[8] E. Schlömann, J. Appl. Phys. **35**, 159 (1964).
[9] R. W. Damon and H. van de Vaart, Phys. Rev. Lett. **12**, 583 (1964).
[10] E. Schlömann and R. I. Joseph, J. Appl. Phys. **35**, 167 (1964).
[11] E. Schlömann and R. I. Joseph, J. Appl. Phys. **35**, 2382 (1964).
[12] W. Strauss, J. Appl. Phys. **35**, 1022 (1964).
[13] W. Strauss, IEEE Trans. Ultrason. Eng. **11**, 85 (1964).
[14] R. W. Damon and H. van de Vaart, J. Appl. Phys. **36**, 3453 (1965).
[15] W. Strauss, Proc. IEEE **53**, 1485 (1965).
[16] E. Schlömann, R. I. Joseph, and T. Kohane, Proc. IEEE **53**, 1495 (1965).
[17] R. W. Damon, B. A. Auld, and W. Strauss, J. Appl. Phys. **37**, 983 (1966).
[18] R. W. Damon and H. van de Vaart, J. Appl. Phys. **37**, 2445 (1966).
[19] R. W. Biereg, R. I. Joseph, and E. Schlömann, IEEE Trans. Ultrason. Eng. **SU-13**, 82 (1966).
[20] W. Strauss, J. Appl. Phys. **36**, 118 (1965).
[21] F. R. Morgenthaler, IEEE Trans. Magn. **13**, 1252 (1977).
[22] M. Tsutsumi, Y. Masaoka, T. Ohira, and N. Kumagai, Appl. Phys. Lett. **35**, 204 (1979).
[23] Yu. I. Bespyatykh, V. I. Zubkov, and V. V. Tarasenko, Zh. Tekh. Fiz. **50**, 140 (1980) [Sov. Phys. Tech. Phys. **25**, 82 (1980)].
[24] D. D. Stancil and F. R. Morgenthaler, IEEE Trans. Magn. **16**, 1156 (1980).
[25] Y. Masaoka, M. Tsutsumi, T. Ohira, and N. Kumgai, Denshi Shashin Gakkaishi **63**, 68 (1980); [Electron. Commun. Jpn. **63**, 68 (1980)].
[26] F. R. Morgenthaler, J. Appl. Phys. **53**, 2652 (1982).
[27] D. D. Stancil and F. R. Morgenthaler, J. Appl. Phys. **54**, 1613 (1983).
[28] M. Tsutsumi, T. Sakurai, and N. Kumagi, IEEE MTT-S Int. Microwave Symp. Dig. **84**, 351 (1984).
[29] M. Tsutsumi, K. Tanaka, and N. Kumgai, IEEE Trans. Magn. **22**, 853 (1986).
[30] A. V. Vashkovskiy, A. V. Stal'makhov, and B. V. Tyulyukin, Pis'ma Zh. Tekh. Fiz. **14**, 1294 (1998)[Sov. Tech. Phys. Lett. **14**, 565 (1988)].
[31] A. V. Vashkovskii, V. I. Zubkov, E. G. Lokk, and V. I. Shcheglov, Radiotekh. Elektron. (Moscow) **1**, 18 (1991)[Sov. J. Commun. Technol. Electron. **36**, 53 (1991)].
[32] A. V. Vashkovskiy, V. I. Zubkov, E. G. Lokk, and V. I. Shcheglov, Radiotekh. Elektron. (Moscow) **5**, 818 (1993)[Sov. J. Commun. Technol. Electron. **38**, 1 (1993)].
[33] A. V. Vashkovskiy, V. I. Zubkov, E. G. Lokk, and V. I. Shcheglov, Radiotekh. Elektron. (Moscow) **40**, 313 (1995)[Sov. J. Commun. Technol. Electron. **40**, 71 (1995)].
[34] A. V. Vashkovskiy, V. I. Zubkov, E. G. Lokk, and V. I. Shcheglov, Radiotekh. Elektron. (Moscow) **40**, 950 (1995)[Sov. J. Commun. Technol. Electron. **40**, 84 (1995)].
[35] M. Tsutsumi and V. Priye, IEEE Trans. Magn. **32**, 4171 (1996).
[36] A. V. Vashkovskiy and E. G. Lokk, Radiotekh. Elektron. (Moscow) **46**, 1257 (2001)[Sov. J. Commun. Technol. Electron. **46**, 1163 (2001)].
[37] S. O. Demokritov, A. A. Serga, A. André, V. E. Demidov, M. P. Kostylev, B. Hillebrands, and A. N. Slavin, Phys. Rev. Lett. **93**, 047201 (2004).
[38] M. Wu, M. A. Kraemer, M. M. Scott, C. E. Patton, and B. A. Kalinikos, Phys. Rev. B **70**, 054402 (2004).
[39] J. M. Nash, C. E. Patton, and P. Kabos, Phys. Rev. B **51**, 15079 (1995).
[40] S. M. Rezende and F. R. Morgenthaler, Appl. Phys. Lett. **10**, 184 (1967).
[41] S. N. Dunaev and Y. K. Fetisov, IEEE Trans. Magn. **29**, 3449 (1993).
[42] Y. K. Fetisov, IEEE Trans. Magn. **29**, 3455 (1993).

Downloaded 26 Aug 2008 to 129.82.140.121. Redistribution subject to AIP license or copyright; see http://jap.aip.org/jap/copyright.jsp